Chemical Physics Letters 612 (2014) 162–166

Contents lists available at ScienceDirect

Chemical Physics Letters

journal homepage: www.elsevier.com/locate/cplett

Spectroscopic signature for ferroelectric ice

Marek J. Wójcik*, Maciej Gług, Marek Boczar, Łukasz Boda

Faculty of Chemistry, Jagiellonian University, Ingardena 3, 30-060 Krakow, Poland

ARTICLE INFO

Article history:
Received 23 May 2014
In final form 7 August 2014
Available online 14 August 2014

ABSTRACT

Various forms of ice exist within our galaxy. Particularly intriguing type of ice – 'ferroelectric ice' was discovered experimentally and is stable in temperatures below 72 K. This form of ice can generate enormous electric fields and can play an important role in planetary formation. In this letter we present Car–Parrinello simulation of infrared spectra of ferroelectric ice and compare them with spectra of hexagonal ice. Librational region of the spectra can be treated as spectroscopic signature of ice XI and can be of help to identify ferroelectric ice in the Universe.

1. Introduction

In the outer solar system, most water ice exists in a crystalline phase [1,2]. Various forms of ice have been found in our galaxy, from interstellar clouds to comets, moons and planets. Infrared observation provides evidence that crystalline ice exists on Pluto's satellite [3]. Below 200 MPa, crystalline ice has two kinds of structure, which are named ice Ih and ice XI. Whether or not ice in the outer solar system exists as ice XI is a question that has attracted scientific interest, because ice XI is ferroelectric. Long-range electrostatic forces, caused by the ferroelectricity, might be an important factor for planet formation [4,5]. Recent studies concerning ice films suggest that a millimeter-sized ferroelectric ice particle has a 10 000 V charge and unusual properties for planetary formation [4,5]. Ice sheets with a thickness of several kilometers on outer planets and the satellites should become a huge source for an electric field because each crystal grain will be similarly aligned due glacial flows like in the polar ice sheets on Earth [6]. The existence of ice XI on Pluto and Charon [7] and the formation of ice XI in space have been predicted [4]; however, from infrared observations it is not clear whether ice XI exists or not.

Protons of ice under high-pressure become readily ordered upon cooling [8]. For an ice doped with 0.1 M KOH, Kawada [9] proposed the existence of a transition from ice Ih to a structure with ordered protons, ice XI. The KOH molecules are ionized, and the OH^- ions, which replace H_2O sites in the ice are considered to increase the mobility of the protons and shorten the transition time. Using this method Fukazawa et al. [6] created samples of ice XI which exists in the narrow temperature range 57–66 K [6]. This is the temperature range at the surfaces of the outer planets of the solar system – Uranus, Neptune and Pluto, their satellites and rings, and rings and moons of Saturn. Analyzing the neutron diffraction pattern the existence of ice XI in the laboratory conditions was proved [6]. The growth of ice XI in time in KOD-doped ice is a matter of hours compared with astronomical timescale for the proton ordering in pure ice, estimated for thousands of years [6].

Infrared spectroscopy is the primary way to detect the emission and absorption lines of most of the molecules as well as numerous atoms and ions in space. Spectrometers onboard infrared missions, and the Infrared Space Observatory (ISO), as well as near-infrared spectra from ground based observatories, have led to the discovery of hundreds of atoms and molecules in many different regions of space. Infrared spectroscopy can provide information about environments which are hidden from optical view, such as regions of star formation and the center of our galaxy. Infrared spectral studies are providing information on the role of interstellar molecules in the formation of stars and planets. For example, infrared spectroscopy has shown that water is abundant in many regions of space, mostly in its crystalline form – ice. Of special importance is ice XI, the structural variant of commonly known ice Ih, due to its ferroelectric properties, which could be additional factor in planet formation processes.

Infrared spectroscopy can be very useful tool for detection of presence of ice XI in the Universe, therefore there is a need to define distinct spectroscopic features which differ infrared spectra of ice Ih and ice XI. In this letter we present results of Car–Parrinello molecular dynamics (CPMD) calculations [10] of infrared spectra of ferroelectric ice XI and compare them with simulated spectra of ice Ih. CPMD calculations have recently become a popular tool for interpretation of infrared spectra of hydrogen-bonded systems [11–22].

* Corresponding author.
E-mail address: wojcik@chemia.uj.edu.pl (M.J. Wójcik).

http://dx.doi.org/10.1016/j.cplett.2014.08.018
0009-2614/

Ice Ih is the hexagonal crystal form of ice. The oxygen atoms form tetrahedral lattice and protons are arranged randomly in accordance with the ice rule [23,24]. Water molecules in ice Ih form four randomly directed hydrogen bonds. Despite proton disorder, hexagonal ice belongs to the $P6_3/mmc$ symmetry space group, due to the distribution of oxygen atoms. There is a small deviation from ideal hexagonal symmetry, as the unit cell is 0.3% shorter in the *c*-direction [25–27]. The crystal structure of ice Ih is not perfect, because of lack of translational symmetry. The unit cell contains four water molecules, however in present calculations, in order to better simulate spectra, we considered eight water molecules.

Ice XI is the proton-ordered form of hexagonal ice. Randomly directed hydrogen bonds in ice Ih change to an ordered arrangement of hydrogen bonds at low temperatures. This process becomes more effective with increased pressure [28]. Electronic structure calculations show very small energetic differences [29–31]. The energy for ice XI is about 0.02–0.016 kcal/mol lower than that of ice Ih. Ice XI should naturally form when ice Ih is cooled below 72 K, where ice XI exists as a stable form, the process which takes thousands of years [6]. The low temperature required to achieve this transition is correlated with the relatively low energy difference between the two structures. Ice XI has an orthorhombic structure with the space group $Cmc2_1$ containing eight water molecules per unit cell. Ice XI is ferroelectric and its ferroelectric properties have been experimentally demonstrated in monolayer thin films [4] and in nano-confined regions.

Features of the infrared spectrum of ice XI became better known due to theoretical studies performed in our laboratory which are presented in this letter.

2. Computational methods

We considered several structures of ice in our calculations [29,30]. Geometry optimizations and vibrational frequency calculations were performed to characterize the key stationary points on the potential energy surface (PES) for unit cell of ice. We have also performed a vibrational analysis of the optimized crystal structures. The calculations were performed using Car–Parinello molecular dynamics program package [32].

Three-dimensional periodicity was fully implemented in our calculation. The CPMD simulations were carried out in the unit cells fixed to the experimentally determined size and taking into account only the positions of atoms. The BLYP density functional [33], together with a plane-wave basis set, with a kinetic energy cutoff of 240 Ry, were used in the simulations. The Goedecker atomic pseudopotentials [34] were used for the treatment of the core electrons. The fictitious orbital mass was set to 300 a.u. The simulations were performed for two temperatures 4 K and 40 K for ice XI and 60 K for ice Ih, by means of Nosé thermostat. The molecular dynamics time step was set to 1.5 a.u. In calculations there were 331 000 steps, the first 71 000 ones were cut. The total simulation time for each structure was 12.00 ps.

The vibrational spectra were calculated using Fourier transformation of the dipole autocorrelation function obtained from the dipole trajectories generated by the CPMD simulations, facilitated by the scripts of Kohlmeyer [35]. The dipole dynamics was calculated using the maximally localized Wannier functions of the Vanderbilt type [36]. From time dependence of the dipole moment, the function of the product of the absorption coefficient with the refraction index was calculated as a function of a wavelength. In last step we used procedure, based on Krammers–Kronig relation between electric susceptibility and light refraction index, to extract the absorption coefficient as a function of wavelength from the product of the absorption coefficient with the refraction index. This function directly translates into the shape of the infrared absorption band.

Table 1
Optimized geometry of water molecules in the crystal of ice XI.

Molecule	Bond [Å]		Bond [Å]		Angle [°]	
1	H1—O1	0.995	H3—O1	0.996	H1—O1—H3	106.33
2	H1—O1	0.995	H3—O1	0.996	H1—O1—H3	106.33
3	H2—O2	0.999	H2—O2	0.999	H2—O2—H2	107.75
4	H2—O2	0.999	H2—O2	0.999	H2—O2—H2	107.75
5	H1—O1	0.995	H3—O1	0.996	H1—O1—H3	106.33
6	H1—O1	0.995	H3—O1	0.995	H1—O1—H3	106.33
7	H2—O2	0.999	H2—O2	0.999	H2—O2—H2	107.75
8	H2—O2	0.999	H2—O2	0.999	H2—O2—H2	107.75

3. Results and discussion

3.1. Geometry analysis

There are 16 crystallographic non-equivalent proton-ordered configurations of ice Ih, shown in Figure 1, with an orthorhombic structure of eight water molecules per unit cell [29,30], however electronic structure calculations show very small energetic differences (0.02–0.016 kcal/mol) between these structures. The $Cmc2_1$ structure (structure A) is the most stable and corresponds to ice XI. In calculations of spectra of ice Ih we considered only five structures of 16 possible, because these structures were invariant during simulation process, whereas in the remaining 11 unit cells significant changes in their structures were observed, i.e. proton transfer between two neighboring molecules. All 16 structures satisfied ice rules in the simulation process. Because of changes in the structures in the 11 unit cells, it was impossible to obtain IR spectra for those structures, therefore they were not considered in the present calculations of the IR spectra The theoretical infrared spectra of ice Ih were obtained as the average of spectra for all five structures, including that of ice XI, whereas the spectrum of ice XI was obtained for the its own structure.

The results of optimization procedure, which was done prior to dynamical calculations, are listed in Table 1. Calculated equilibrium bond lengths and angles slightly exceed their initial values (by about 0.03 A and 2–3° respectively). Analyzing the data from Table 1 it can be noticed that within the unit cell there are two sets of molecules with similar geometry (set I: 1, 2, 5, 6 and set II: 3, 4, 7, 8). The differences between sets are mainly caused by various molecular neighborhoods which are responsible for the presence of slightly different hydrogen bonds. Based on the trajectories of the nuclei, obtained from Car–Parrinello molecular dynamics simulations, the average bond lengths and bond angles were calculated in the next step at temperatures 4 K and 40 K. It was observed that equilibrium inter-atomic distances are almost equal to the averaged ones. Some of the bond lengths at 4 K are slightly shorter than at 40 K. In the case of the bond angles, simulation at 4 K gives values larger than the equilibrium ones by ~0.5° for the set I and ~0.2° for set II. At 40 K the respective bond angles are larger by ~0.8° and ~0.2° than the equilibrium values. At higher temperatures two sets of molecules tend to get similar because the influence of molecular neighborhoods on the geometry of water molecules becomes smaller.

3.2. Infrared spectra of ice Ih and ice XI

Simulation of infrared spectra of ice Ih at 60 K and ice XI at 4 and 40 K, using Car–Parrinello method of molecular dynamics, is presented in Figure 2. Band frequencies are listed in Table 2 and compared with the available experimental data for ice Ih.

In order to assign peaks to particular sets of water molecules, the power spectra of atoms belonging to different atomic groups were calculated. The three prominent bands are present in the IR

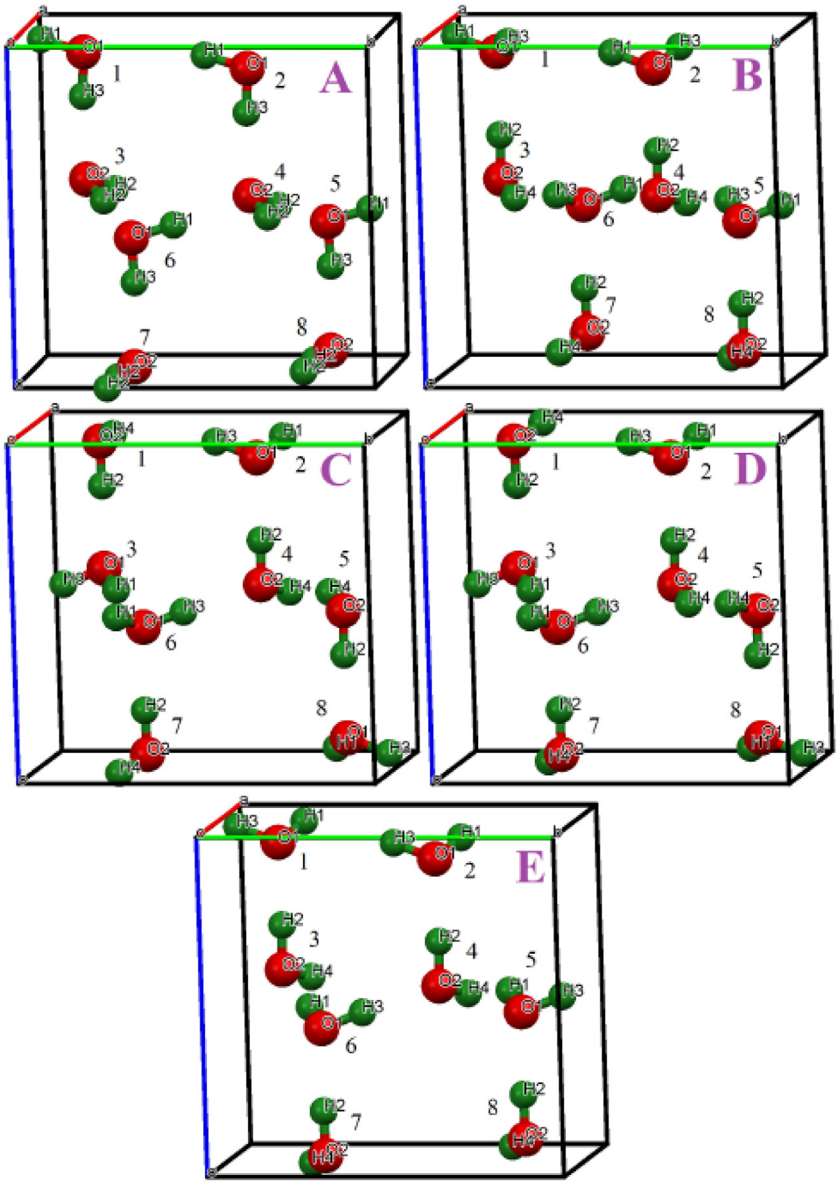

Figure 1. The five unit cells with eight water molecules chosen for the calculations. Symmetry space groups are: (A) $Cmc2_1$, (B) $Pbn2_1$, (C) $P2_12_12_1$, (D) $P2_12_12_1$, (E) $C1c1$. The (A) structure corresponds to ice XI.

Table 2
Calculated and experimental infrared frequencies if ice Ih and XI.

Calculated			Experimental [37]	
Ice Ih at 60 K	Ice XI at 4 K	Ice XI at 40 K	Ice Ih at ~100 K	
3255	3255	3260	3380–30	sh s
	3210			
3150	3120	3130	3220 ± ~5	s
3080				
2925	3030	3025	3150–10	sh s
	3000			
~2240	–	2365	2266 ± ~20	vb w
		2200		
1600	1660	1670	1650 ± ~30	vb w
	1575	1575		
790–1080	1010	1000	900	sh
	940	930	840	s
–	705	700	770	sh
620	625	630	660	sh
445	460	–	555	sh
390				

sh – shoulder, s – strong, m – medium, w – weak, v – very, b – broad.

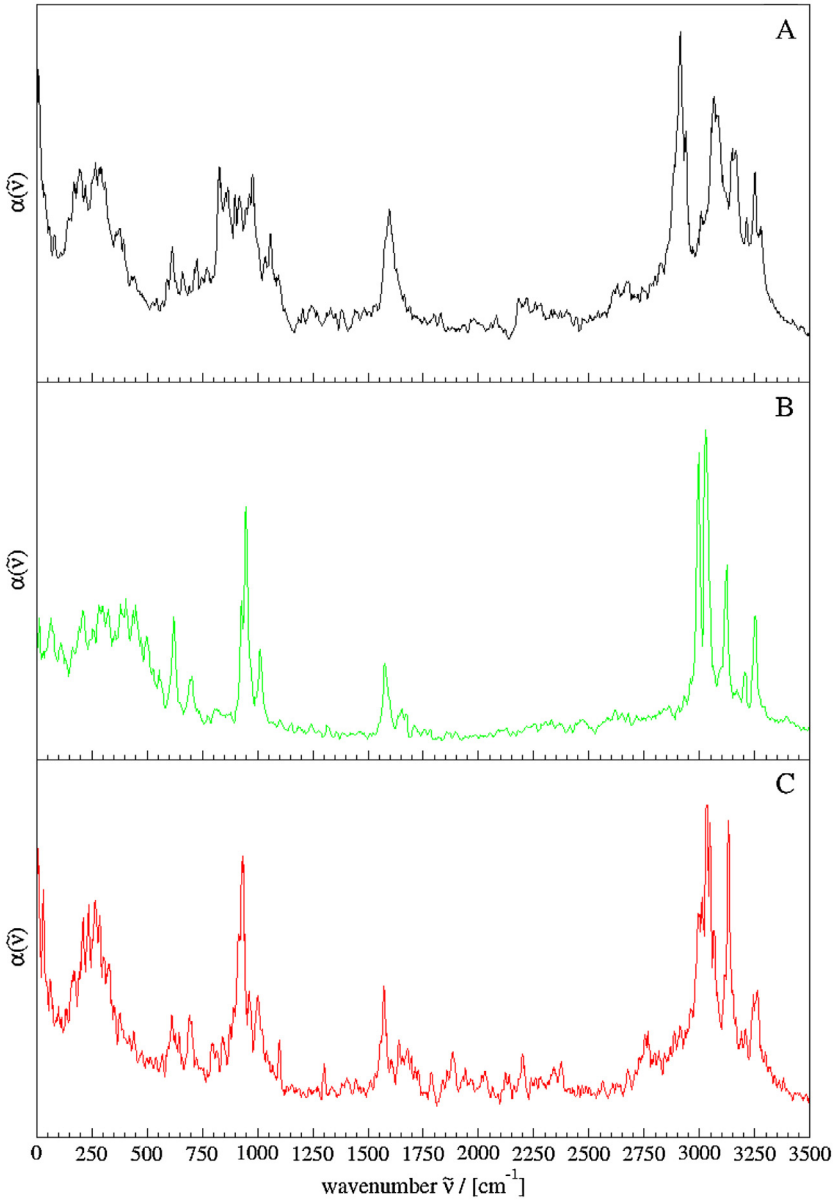

Figure 2. Comparison between theoretical IR spectrum of ice Ih calculated at 60 K (A) and ice XI calculated at 4 K (B) and 40 K (C).

spectra of ice XI at two temperatures 4 K and 40 K: at 600–1100 cm^{-1} formed by the librational mode (ν_L), at 1500–1750 cm^{-1} formed by the HOH bending mode (ν_B), and at 2700–3300 formed by the OH stretching mode (ν_S). Additionally, at 40 K there appear few weak bands in the range 1800–2400 cm^{-1}. They are the overtone of the librational mode ($3\nu_L$) and combination of the bending and librational mode ($\nu_L + \nu_B$) [37]. Increase of temperature does not significantly affect band broadening. At lower temperature the position of the ν_S band is shifted to lower frequency. Such shifts occur in systems with strong hydrogen bonds [38]. This result is also consistent with experimental temperature studies of infrared spectra of ice XI [39].

The simulated spectra of ice Ih and ice XI show many differences. Especially significant is the region of the librational motions of water molecules, presented in Figure 3, because in this region there is a unique large difference in the spectra between ice Ih and ice XI. Librational spectrum of ice Ih has more simple structure with only two bands – one very broad at about 790–1080 cm^{-1} and the second with small intensity at about 620 cm^{-1}. In the case of ice XI the librational spectrum is different – it is composed of two major bands, located at 945 cm^{-1} and 1015 cm^{-1} at temperature 4 K, and at 930 cm^{-1} and 1000 cm^{-1} at temperature 40 K. These bands can be treated as spectroscopic signatures of ice XI.

Our results are in agreement with experimentally measured infrared spectra of KOH-doped ice [39]. Infrared and Raman spectra of ice Ih have been previously calculated using different water–water interaction potentials by Rice et al. [40,41], Wójcik et al. [42] and Skinner et al. [43,44]. Our CPMD simulated spectra of ice Ih are in agreement with these calculations. Recently experimental studies of the Raman spectra of hydrogen-ordered ice have been also reported [45,46]. They showed, similar to the IR studies, that there are distinct differences in the Raman spectra between ices Ih and XI, with ice XI showing much stronger peaks in the translational, librational and in-phase asymmetric stretch regions.

To find distant ice XI in outer space we will need to investigate in detail the librational motions of water molecules on the surface ice on large satellites without an atmosphere. The evidence for ice XI in the doped ice and the simulated infrared bands of ice XI hold

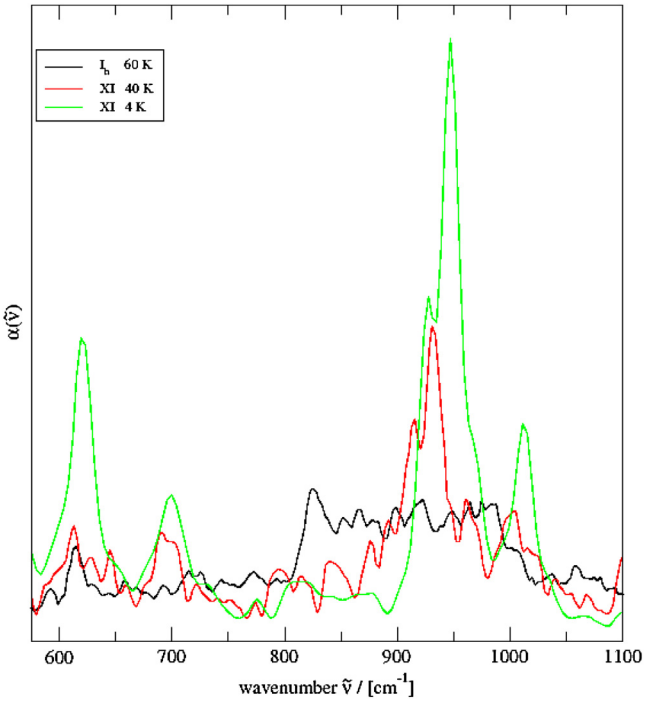

Figure 3. Comparison between librational spectra of ice Ih calculated at 60 K and ice XI calculated at 4 K and 40 K.

out the hope that future telescope and planetary exploration will find huge ferroelectric ice XI in the solar system. Simulated spectra of ice XI can of help in identifying ice XI in the outer solar system.

4. Conclusions

Theoretical infrared spectra of ice Ih and ferroelectric ice XI were calculated using Car–Parrinello molecular dynamics. The librational region exhibits especially large differences in the simulated spectra of ice Ih and ice XI. Theoretical IR spectra of ice XI can be a useful tool for analysis of experimental data obtained by IR telescopes to investigate presence of ferroelectric ice in the Universe.

Acknowledgements

This research was supported in part by PL-Grid Infrastructure.

References

[1] A. Kouchi, T. Yamamoto, T. Kozasa, J.M. Greenberg, Astron. Astrophys. 290 (1994) 1009.
[2] T.L. Roush, J. Geophys. Res. 106 (2001) 33315.
[3] M.E. Brown, W.M. Calvin, Science 287 (2000) 107.
[4] M.J. Iedema, M.J. Dresser, D.L. Doering, J.B. Rowland, W.P. Hess, A.A. Tsekouras, J.P. Cowin, J. Phys. Chem. B 102 (1998) 9203.
[5] H. Wang, R.C. Bell, M.J. Iedema, A.A. Tsekouras, J.P. Cowin, Astrophys. J. 620 (2005) 1027.
[6] H. Fukazawa, A. Hoshikawa, Y. Ishii, B.C. Chakoumakos, J.A. Fernandez-Baca, Astrophys. J. 652 (2006) L57.
[7] W.B. McKinnon, A.M. Hofmeister, BAAS 37 (2005) 732.
[8] W.F. Kuhs, J.L. Finney, C. Vettier, D.V. Bliss, J. Chem. Phys. 81 (1984) 3612.
[9] S. Kawada, J. Phys. Soc. Jpn. 32 (1972) 1442.
[10] R. Car, M. Parrinello, Phys. Rev. Lett. 55 (1985) 2471.
[11] S.S. Iyengar, M.K. Petersen, T.J.F. Day, C.J. Burnham, V.E. Teige, G.A. Voth, J. Chem. Phys. 123 (2005) 084309.
[12] J. Mavri, A. Jezierska, J.J. Panek, A. Koll, J. Chem. Phys. 126 (2007) 205101.
[13] J. Stare, J.J. Panek, J. Eckert, J. Grdadolnik, J. Mavri, D. Hadži, J. Phys. Chem. A 112 (2008) 1576.
[14] P. Durlak, Z. Latajka, S. Berski, J. Chem. Phys. 131 (2009) 024308.
[15] P. Durlak, Z. Latajka, Chem. Phys. Lett. 477 (2009) 249.
[16] J. Mavri, G. Pirc, J. Stare, J. Chem. Phys. 132 (2010) 224506.
[17] G. Pirc, J. Stare, J. Mavri, J. Chem. Phys. 132 (2010) 224506.
[18] R. Vianello, J. Stare, J. Mavri, J. Grdadolnik, J. Zidar, Z.B. Maksic, J. Phys. Chem. B 115 (2011) 5999.
[19] P. Durlak, Z. Latajka, J. Mol. Model. 17 (2011) 2159.
[20] J. Kwiendacz, M. Boczar, M.J. Wójcik, Chem. Phys. Lett. 501 (2011) 623.
[21] M. Brela, J. Stare, G. Pirc, M. Sollner-Dolenc, M. Boczar, M.J. Wójcik, J. Mavri, J. Phys. Chem. B 116 (2012) 4510.
[22] M.Z. Brela, M.J. Wójcik, M. Boczar, R. Hashim, Chem. Phys. Lett. 558 (2013) 88.
[23] J.D. Bernal, R.H. Fowler, J. Chem. Phys. 1 (1933) 515.
[24] L. Pauling, J. Am. Chem. Soc. 57 (1935) 2680.
[25] W.H. Barnes, Proc. R. Soc. Lond. Ser. A 125 (1929) 670.
[26] C.J. Burnham, J. Li, C.M. Leslie, J. Chem. Phys. 101 (1997) 6192.
[27] S.W. Paterson, H.A. Levy, Acta Crystallogr. 10 (1957) 70.
[28] A.H. Castro Neto, P. Pujol, E. Fradkin, Phys. Rev. B 74 (2006) 024302.
[29] J.L. Kuo, S.J. Singer, Phys. Rev. E 67 (2003) 016114.
[30] T.K. Hirsch, L. Ojamae, J. Phys. Chem. B 108 (2004) 15856.
[31] C. Knight, S.J. Singer, J.-L. Kuo, T.K. Hirsch, L. Ojamäe, M.L. Klein, Phys. Rev. E 73 (2006) 056113.
[32] CPMD, Copyright IBM Corp 1990–2006, Copyright MPI für Festkörperforschung Stuttgart 1997–2001.
[33] C.T. Lee, W.T. Yang, W.T. Parr, Phys. Rev. B 37 (1988) 785.
[34] S. Goedecker, K. Maschke, Phys. Rev. A 45 (1992) 88.
[35] H. Forbert, A. Kohlmeyer, Fourier, v 1.1, 2002–2008.
[36] N. Marzari, D. Vanderbilt, Phys. Rev. B 56 (1997) 12847.
[37] J.E. Bertie, E. Whalley, J. Chem. Phys. 40 (1964) 1637.
[38] J.E. Bertie, E. Whalley, J. Chem. Phys. 40 (1964) 1646.
[39] M. Arakawa, H. Kagi, H. Fukazawa, Astrophys. J. Suppl. 184 (2009) 361.
[40] M.S. Bergren, S.A. Rice, J. Chem. Phys. 77 (1982) 583.
[41] S.A. Rice, M.S. Bergren, A.C. Belch, G. Nielson, J. Phys. Chem. 87 (1983) 4295.
[42] M.J. Wójcik, K. Szczeponek, S. Ikeda, J. Chem. Phys. 117 (2002) 9850.
[43] F. Li, J.L. Skinner, J. Chem. Phys. 132 (2010) 204505.
[44] F. Li, J.L. Skinner, J. Chem. Phys. 133 (2010) 244504.
[45] K. Abe, T. Shigenari, J. Chem. Phys. 134 (2011) 104506.
[46] T. Shigenari, K. Abe, J. Chem. Phys. 136 (2012) 174504.